

Doi: <http://dx.doi.org/10.1590/1809-4430-Eng.Agric.v41n2p181-195/2021>

PEACH PIT CHEMICALLY TREATED BIOMASS AS A BIOSORBENT FOR METFORMIN HYDROCHLORIDE REMOVAL: MODELING AND SORPTION MECHANISMS

Liliane Hellmann¹, Ana P. de O. Schmitz^{2*}, Aparecido N. Módenes¹,
Camila L. Hinterholz¹, Camila de A. Antonioli²

^{2*}Corresponding author. Federal Technological University of Paraná/ Francisco Beltrão - PR, Brazil. E-mail: anapoliveira@utfpr.edu.br | ORCID: <https://orcid.org/0000-0002-6318-6813>

KEYWORDS

biosorption,
metformin
hydrochloride, peach
pit, kinetic modeling,
equilibrium modeling

ABSTRACT

In this work, the potential of peach pit biosorption in the removal of the drug metformin hydrochloride from water is evaluated. Experiments are carried out in a closed batch system to evaluate the effect of the solution pH (2–10), temperature (25, 35 and 45 °C), stirring (100, 150 and 200 rpm) and chemical treatments. During the study, biosorbent characterization, kinetic tests, equilibrium tests and thermodynamic parameter calculations are performed. The operating conditions that show the best results for both the raw biosorbent and the biosorbent submitted to acid, basic and acid followed by basic treatments with removal capacities of 3.17, 10.83, 18.10 and 49.14 mg g⁻¹, respectively, are pH 7, 25 °C and 100 rpm, which result in an equilibrium time of 12 h. In the kinetic study, the pseudo-second-order model represents the best fit for the experimental data, while the Langmuir model best represents the equilibrium data. The biomasses submitted to chemical treatments show a significant increase in drug removal capacity related to the raw biosorbent, with the best maximum absorption of 82.54±1.34 mg g⁻¹ achieved after the application of the acid followed by basic treatment. These results show that peach pit has potential to be used as a low-cost biosorbent to remove drugs from water.

INTRODUCTION

The worldwide environmental impact and large number of emerging contaminants detected in surface waters have become major global concerns. Such contaminants come, in general, from industrial waste that generates serious problems of water pollution for containing elements, which above certain concentrations can be toxic to humans and the environment. The presence of drugs, pesticides and hormones in water can generate high risks to human health due to their accumulation, as they can, in addition to changing the normal level of hormones in humans and animals, create microbial resistance to drugs (Jean et al., 2012; Álvarez-Torrellas et al., 2016; Bartrons & Penuelas, 2017). In recent years, the significant increase in the consumption of these compounds and their effects on the ecosystem and human body have received significant attention, particularly regarding their effective elimination.

Metformin hydrochloride, a potent anti-hyperglycemic agent that is currently recommended for oral therapy in the treatment of type 2 diabetes, is an example drug that is introduced into the environment in greater volumes, since a large part of the medication ingested by an individual gets excreted in urine, unchanged or slightly modified, as a result of incomplete absorption by the human body. Drug residues, which are not metabolized by the human body and, thus, excreted in urine, are discharged into domestic sewage and then sent to the sewage treatment units of sanitation companies, where no specific treatment for this type of substance (Niemuth et al., 2015) is provided. In addition, drug residues may come from effluents from pharmaceutical industries, which due to the lack of specific legislation requiring maximum disposal concentrations, discharge residues into the environment without proper treatment. Thus, the limit concentrations of toxicity may be exceeded (Larsson, 2014).

¹ West Paraná State University/ Toledo - PR, Brazil.

² Federal Technological University of Paraná/ Francisco Beltrão - PR, Brazil.

Area Editor: Airton Kunz

Received in: 8-10-2020

Accepted in: 12-22-2020



Bearing in mind that conventional treatments are not able to remove or degrade these pollutants efficiently, treatment technologies are required (Carmalin & Lima, 2018). Among the various possible techniques, adsorption methods are very popular and effective due to their environmental and economic benefits (Módenes et al., 2015a; Inyang & Dickenson, 2015; Tan et al., 2015; Rigueto et al., 2020).

Bioresidues from the agricultural and food industries have been used as potential biosorbents in the treatment of water and effluents (Espinoza-Quiñones et al., 2010; Módenes et al., 2015a; Módenes et al., 2015b; Scheufele et al., 2016; Ribeiro et al., 2018; Shakoor et al., 2019; Scheufele et al., 2019; Bazarin et al., 2019; Módenes et al., 2019), due to them being natural resources, as well as renewable and economically viable (Rezaee et al., 2008). However, further research is needed to explore different biosorbents, as well as their efficiency in the drug adsorption process.

Peach pit, a residue from peach processing, has been applied as an adsorbent in the removal of textile dyes (Muñoz-González et al., 2008; Markovic et al., 2015; Yan et al., 2018), metals (Maldonado et al., 2016; Yan et al., 2018) and drugs (Conrado, 2019; Álvarez-Torrelas et al., 2015). In addition, this biosorbent has been shown to be an excellent alternative of treatment to minimizing the impact caused by the discharge of effluents, with its use promoting the use of solid waste, which is often discarded in the environment due to its slow decomposition and high stiffness.

In this sense, the objective of this study is to use a solid agricultural and industrial residue with peach pit to remove metformin hydrochloride from water by evaluating the appropriate operational parameters (pH, temperature and stirring) for both the raw biosorbent (RW) and the biosorbent submitted to acid (AT), basic (BT) and acid followed by basic (ABT) treatments. Additionally, a thermodynamic, kinetic and equilibrium study is performed, which provides estimations of some of the main kinetic and equilibrium models found in the literature.

MATERIAL AND METHODS

Residue from peach processing

The Agate peach variety used by peach processing agribusinesses in the southwestern region of Paraná, Brazil, undergoes the process of cutting and ginning during the production of peaches into syrup and jelly. The peach pit discarded in this process was collected and dried for 2 months in open air. After this period, it was washed with running water, rinsed with distilled water, dried in an oven at 40 °C, crushed and sieved to a particle size of 0.04 to 1 mm.

Analysis and preparation of solutions and biomass

The solutions were prepared from the dissolution of the pharmaceutical ingredient (metformin hydrochloride) in distilled water. The drug concentration analyzes were performed using ultraviolet-visible (UV-Vis) spectrophotometry in a 200 to 700 nm range (Shimadzu, Model UV 1800). To determine the concentration of the drug solution, a calibration curve was constructed with concentrations from 2 to 20 mg L⁻¹ ($Conc = 12.131Abs$; $R^2 = 0.998$), which is linearly related to the concentration of the drug solution with the corresponding absorbance.

Chemical treatment of peach pit

The acid treatment was carried out by adding 10 g of the ground peach pit in 1 L of 1 mol L⁻¹ phosphoric acid solution, with the temperature controlled at 80 °C and 100 rpm stirring with a magnetic stirrer for 30 min. A similar procedure was performed for the basic treatment, in which a 1 mol L⁻¹ sodium hydroxide (NaOH) solution was maintained under stirring of 100 rpm (magnetic stirrer) at room temperature for 30 min. After each chemical treatment (acid and basic), the solid part was separated from the liquid, rinsed with distilled water until reaching neutral pH and then dried in an oven (at 100 and 40 °C for the acid and basic treatments, respectively). In addition, a basic treatment was carried out on a portion of the biomass treated with phosphoric acid.

Determination of point of zero charge (pHpzc)

The pHpzc of the biosorbent is an important resource to understand the adsorption process. This parameter corresponds to the pH at which the surface charge of the biosorbent is zero. According to Davranche et al. (2003), the surface of the material can present a positive, negative or zero charge, based on the pH of the surrounding solution, and may behave like an anion or cation exchanger. Cation adsorption is favored at pH > pHpzc, while anion adsorption is favored at pH < pHpzc.

To determine the pH at which the surface charge of the biosorbent was zero (pHpzc), the methodology proposed by Davranche et al. (2003) and described in detail by Módenes et al. (2013) was used. Based on this methodology, two flasks containing a suspension of 5 g of adsorbent and 100 mL of NaNO₃ (0.1 mol L⁻¹) were prepared. Both suspensions were then titrated, one with HNO₃ (0.1 mol L⁻¹) and the other with NaOH (0.1 mol L⁻¹). The amount of acid and base necessary to reach each pH value (in a pH range between 2 and 12) was recorded. The net charge on the biosorbent surface was calculated according to [eq. (1)]:

$$q = \frac{C_A - C_B + [OH^-] + [H^+]}{C_S} \quad (1)$$

Where:

C_A and C_B - acid and base concentration (mol L⁻¹), respectively;

C_S - mass per volume of biosorbent in solution (g L⁻¹),

$[OH^-]$ and $[H^+]$ - hydroxyl and hydrogen ions in solution (mol L⁻¹), respectively.

Scanning electron microscopy

To assess the biomass surface morphology of RW, AT, BT and ABT, scanning electron microscopy analyzes were obtained using a Hitachi 3000 digital microscope, which consists of the emission of an electron beam by a capillary filament of tungsten by applying a potential difference. For such analyzes, the biosorbent was previously dried at 100 °C, placed on a copper strip and subsequently introduced into the equipment to generate the images that were enlarged 1000 times.

Fourier transform infrared (FTIR) spectroscopy

To verify possible changes in the functional groups caused by the chemical treatment and/or by the adsorption process, FTIR analyzes were performed in both the RW and treated samples, before and after the adsorption of the drug. The KBr tablet methodology was used, with lozenges prepared by the homogeneous mixing and grinding of 1 mg of sample and 99 mg of KBr in a mortar previously dried at 105 °C. Pasturing was carried out with the gradual application of an 8-ton pressure to the mixture for ~5 min. Using a PerkinElmer model Frontier IR system, FTIR spectra were obtained in the range of 4000 to 400 cm⁻¹ with a resolution of 4 cm⁻¹.

Preliminary tests

A set of tests were carried out to evaluate the best operating conditions for the pH (4–10), sorption temperature (25, 35 and 45 °C) and stirring (100, 150 and 200 rpm) in the adsorption of metformin hydrochloride (Table 1). Furthermore, adsorption tests were carried out to verify the effect of chemical treatments on the peach pit sorption capacity to adsorb the drug.

TABLE 1. Experimental design to evaluate the influence of pH, temperature (°C) and stirring (rpm) parameters.

Test	Parameters		
	pH	Temperature (°C)	Stirring (rpm)
1	4	25	100
2	5	25	100
3	6	25	100
4	7	25	100
5	8	25	100
6	9	25	100
7	10	25	100
8	7	25	100
9	7	35	100
10	7	45	100
11	7	25	100
12	7	25	150
13	7	25	200

Preliminary tests were performed in duplicate, with the addition of a mixture of 0.25 g of biosorbent to 50 mL of the drug solution with an initial concentration of 100 mg L⁻¹ in 125 mL flasks under constant stirring (100 rpm) at a controlled temperature for a period of 24 h. After this contact period, the adsorbent solution was separated by centrifugation at 3000 rpm for 10 min. The determination of the initial and post-adsorption concentrations of the solution was performed by UV-Vis spectrophotometry at a wavelength of 233 nm (USP, 2012).

The amount of drug adsorbed by the biosorbent was calculated from the mass balance described in [eq. (2)]:

$$q = \frac{(C_0 - C)V}{m} \quad (2)$$

Where:

$q(t)$ - amount of adsorbed drug (mg g⁻¹);

C_0 and C - initial and final concentration (mg L⁻¹), respectively;

V - volume of solution (L),

m - adsorbent mass (g).

The results were evaluated by means of the analysis of variance (ANOVA), considering the independent variables of pH, temperature and stirring, as well as the dependent variable removal percentage. Statistically significant differences were investigated at a 95% confidence level. For such analyzes, the StatSoft® Inc. Statistica software was used.

Kinetic tests

Kinetic tests were performed using the peach pit (RW, AT, BT and ABT). Based on the results obtained with the preliminary tests, the most appropriate operational conditions for the kinetic study were determined. Therefore, under such sorption conditions (pH 7, 25 °C and 100 rpm), mixtures of 0.25 g of biosorbent and 50 mL of drug solution, with initial concentrations of 100 and 400 mg L⁻¹, were prepared in Erlenmeyer flasks. The mixtures were kept under constant stirring on an orbital shaking table at a controlled temperature of 25 °C for 24 h. Aliquots (vials) were withdrawn at predetermined time intervals (1 to 1440 min) for further analysis with the UV-Vis spectrophotometer.

Equilibrium tests

Equilibrium tests were performed in triplicate under the same operational conditions used in the kinetic tests. In addition, for the ABT sample, equilibrium tests were performed at 25, 35 and 45 °C. The tests were carried out in batches, in Erlenmeyer flasks with a mixture of 0.25 g of biosorbent and 50 mL of drug solution, with concentrations ranging from 5 to 800 mg L⁻¹, and with a contact time of 24 h.

The adsorption capacity of the peach pit was determined in the equilibrium study and the data were further used to adjust isotherm models usually used to express the properties between the adsorbent surface and the affinity with chemical species.

Kinetic modeling

For the adsorption kinetics, the mass transfer between the solid and liquid phases can be described by the pseudo-first-order model proposed by Lagergren (Lagergren, 1898; Ho & McKay, 1999), given in [eq. (3)], where the rate of adsorption is directly proportional to the difference between the current and equilibrium concentrations. If the adsorption depends on the adsorbent-adsorbate interaction, then the process is described by the pseudo-second-order model (Ho & McKay, 2000; Ho, 2004), given by [eq. (4)], where the amount of adsorbate removed is proportional to the square of the difference between the saturation concentration and the drug concentration in the adsorbent.

$$q = q_{eq} \left(1 - e^{-k_1 t}\right) \quad (3)$$

Where:

k_1 - velocity constant (h^{-1}),
 q_{eq} and $q(t)$ - drug removal capacity in the equilibrium and during time t (h), respectively.

$$q = \frac{q_{eq}^2 k_2 t}{1 + q_{eq} k_2 t} \quad (4)$$

Where:

k_2 - velocity constant ($\text{g mg}^{-1} \text{h}^{-1}$).

To verify the possibility that intraparticle diffusion is the mechanism responsible for the diffusion of the drug adsorption process, a model proposed by Weber & Morris (1963), dependent on the square root, was applied, as described in [eq. (5)]. Usually, this model shows three different regions that correspond to the stages of external diffusion, macropores and micropores.

$$q = k_{dif} \sqrt{t} + C \quad (5)$$

Where:

k_{dif} - intraparticle diffusion rate constant ($\text{mg g}^{-1} \text{h}^{-1/2}$);

t - contact time,

C - constant related to the diffusion resistance.

Equilibrium modeling

Based on the relation between the adsorption capacity of the biomass and the equilibrium concentration, the data were evaluated using isotherm models usually applied to biosorption studies, which allow for the evaluation of the nature of the adsorption process. The equations and parameters of the mentioned models are demonstrated as expressed by eqs. (6) - (11):

$$\text{Langmuir (1916): } q_{eq} = \frac{q_{max} b C_{eq}}{1 + b C_{eq}} \quad (6)$$

$$\text{Freundlich (1906): } q_{eq} = k_F (C_{eq})^n \quad (7)$$

$$\text{Redlich & Peterson (1959): } q_{eq} = \frac{k_{rp} C_{eq}}{1 + a_{rp} C_{eq}^g} \quad (8)$$

$$\text{Temkin (1981): } q_{eq} = b \ln(k_T) + b \ln(C_{eq}) \quad (9)$$

Dubinin (1960):

$$q_{eq} = \frac{q_{max,DR}}{\exp \left[\beta_{sDR} \left[RT \ln \left[1 + \frac{1}{C_{eq}} \right] \right]^2 \right]} \quad (10)$$

$$\text{Toth (1971): } q_{eq} = \frac{q_{max,T} b_T C_{eq}}{\left(1 + (b_T C_{eq})^{n_T} \right)^{1/n_T}} \quad (11)$$

Where:

q_{max} - maximum capacity of drug adsorption by the Langmuir isotherm (mg g^{-1});

q_{eq} - equilibrium capacity of drug adsorption (mg g^{-1});

C_{eq} - equilibrium concentration (mg L^{-1});

b - the ratio between the adsorption and desorption rates (mg L^{-1});

k_F - Freundlich constant (mg g^{-1});

n - constant that characterizes the adsorption intensity;

k_{rp} and a_{rp} - Redlich-Peterson parameters, with the respective units L g^{-1} and mg L^{-1} , respectively;

g - exponent of Redlich-Peterson (dimensionless), which must be ≤ 1 ; maximum capacity of drug adsorption by the Langmuir isotherm (mg g^{-1});

B - constant that represents the adsorption heat;

k_T - bonding equilibrium constant (L mg^{-1});

$q_{max,DR}$ - maximum capacity of drug adsorption by the Dubinin-Radushkevich isotherm (mg g^{-1});

β_{sDR} - represents the activity coefficient according to the sorption average energy ($\text{mol}^2 \text{kJ}^{-2}$);

R - constant of ideal gases ($8.314 \text{K}^{-1} \text{mol}^{-1}$);

T - temperature (K);

b_T - Toth constant (L mg^{-1});

n_T - homogeneity parameter, which ranges from 0 to 1.

The estimation of the equilibrium and kinetic model parameters was performed by applying the nonlinear identification procedure in Origin® 8.0 Pro software.

Thermodynamic parameters

After performing the analysis of the temperature effect, the process adsorption thermodynamics were verified. For this analysis, the Gibbs energy (ΔG°), enthalpy (ΔH°) and entropy (ΔS°) of the system were evaluated. The variation in the Gibbs free energy is given by [eq. (12)]:

$$\Delta G^\circ = -RT \ln(K_{eq}) \quad (12)$$

Where:

R - ideal gas constant ($8.314 \text{ mol}^{-1} \text{ K}^{-1}$);

T - system operating temperature (K);

K_{eq} - equilibrium constant.

The relation between the three parameters is given by [eq. (13)]:

$$\Delta G^{\circ} = \Delta H^{\circ} - T\Delta S^{\circ} \quad (13)$$

According to [eq. (13)], the intersection and slope of a line with the ordinate axis provide the enthalpy and entropy values, respectively.

RESULTS AND DISCUSSION

Determination of pHPzc

The behavior of the surface net electrical charge of the biosorbent (RW, AT, BT and ABT), as a function of pH (Figure 1), showed a zone of neutral net surface charge for RW, BT and ABT in a pH range between 6 and 8. For AT, the same pattern occurred at pH ~3, according to Figure 1. The pH values identified below the pHPzc suggest that the surface of the adsorbent behaves as a positive net surface charge (anion adsorption), while for pH values above pHPzc, the adsorbent surface is negative (cation adsorption) (Oliveira et al., 2018).

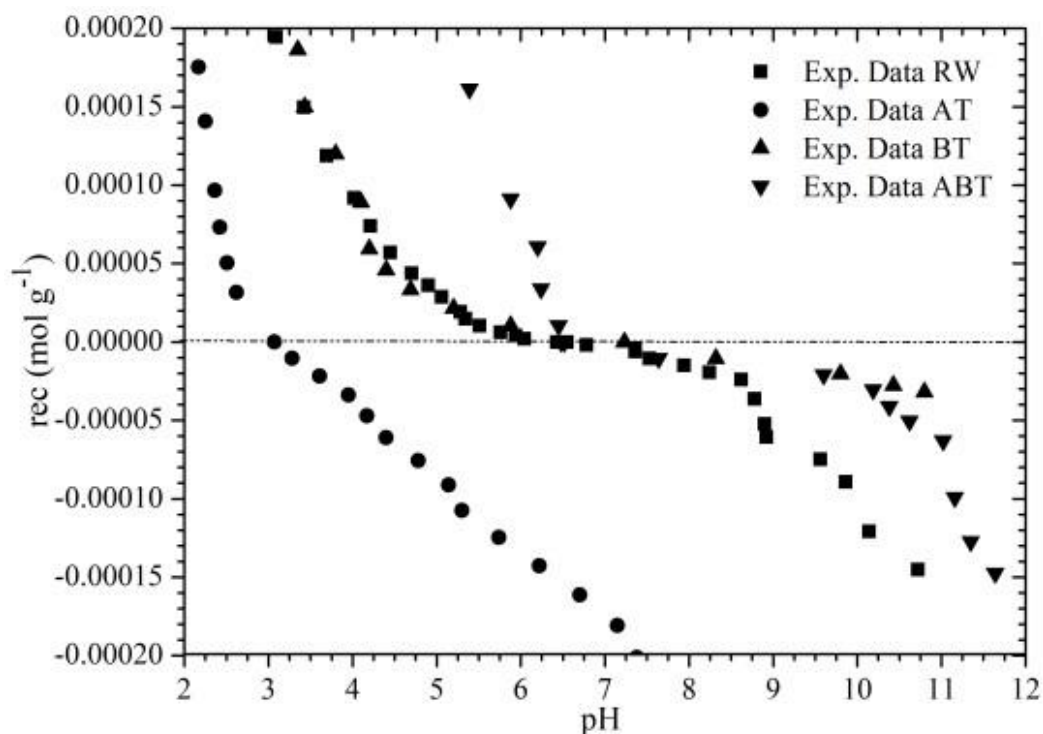


FIGURE 1. Behavior of the net electrical charge for the RW, AT, BT e ABT biosorbent as a function of pH.

Scanning electron microscopy

With the images obtained from the scanning electron microscopy analysis, shown in Figure 2, it is possible to analyze the texture and roughness characteristics of the materials. It is observed that the biomass surfaces for both raw and modified by chemical treatments are irregular and have excellent porosity. It can also be seen that after

chemical treatments (Figures 2(b)-(d)), the structure of the biosorbent subjected to BT and ABT presented a more irregular and heterogeneous surface morphology. This may cause an increase in the capacity of adsorption of the material, since the aim of the activation is to remove compounds that may obstruct the pores, as well as increase the specific surface area in the material.

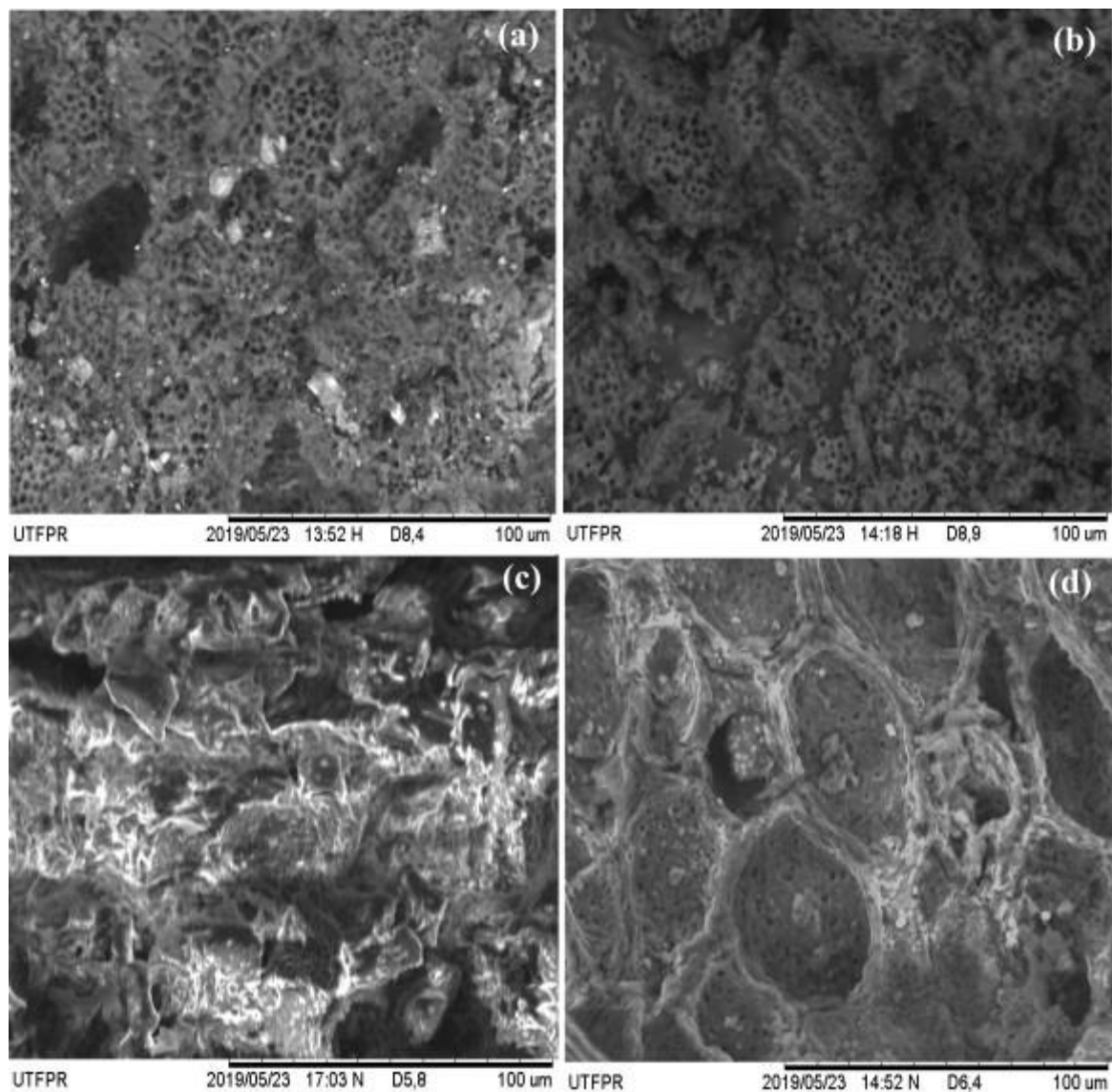


FIGURE 2. Micrographs obtained for biomass with 1000 times magnification: (a) RW, (b) AT, (c) BT and (d) ABT.

FTIR analysis

The possible functional groups present in the structure of the peach pit were characterized by FTIR analysis in the range of $4000\text{--}450\text{ cm}^{-1}$. Figure 3 shows the spectra in a range from $2000\text{ to }800\text{ cm}^{-1}$, where the main

chemical bonds of the functional groups were identified. The structural properties present in the peach pit for both raw and after chemical treatments are located in the region of $1800\text{--}900\text{ cm}^{-1}$, where there is evidence of organic leaching.

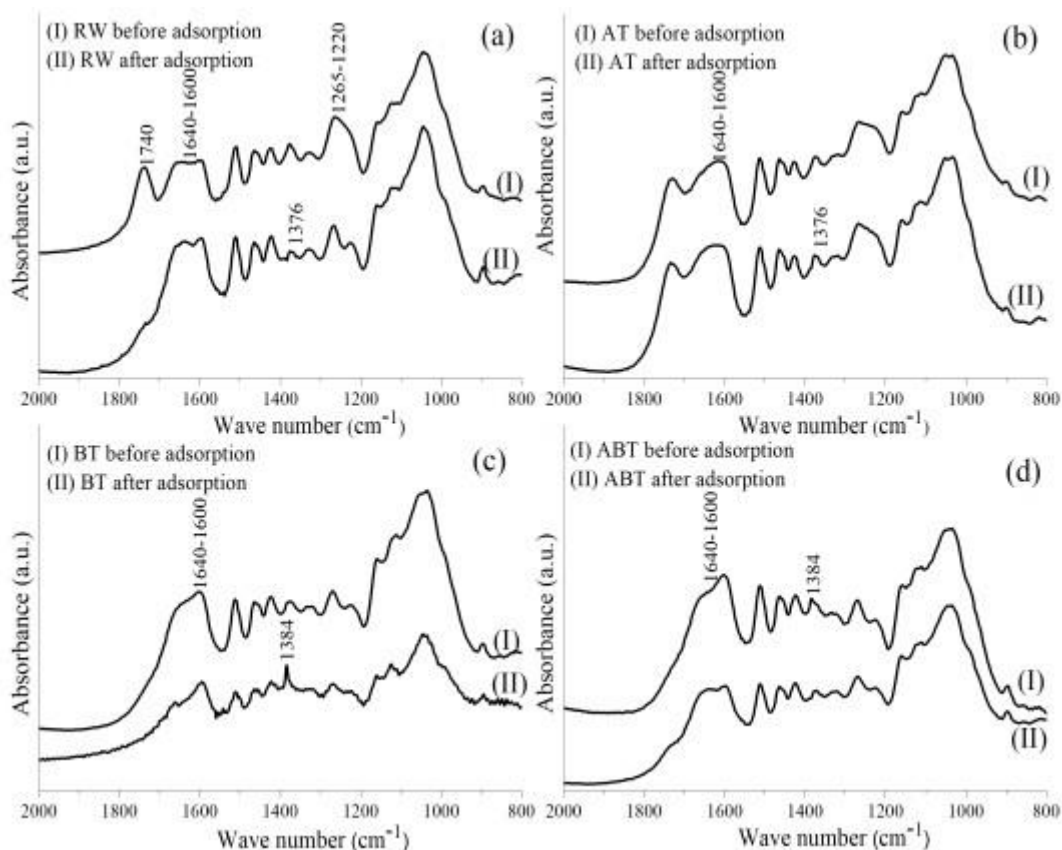


FIGURE 3. Typical infrared spectrum for a samples before and after adsorption process (a) RW, (b) AT, (c) BT and (d) ABT.

At 1740 cm^{-1} , there are considerable changes in the spectra of the biomass submitted to chemical treatments when compared to the raw biosorbent, which indicate carboxylic groups or correspondences for aldehyde, ketone and esters ($\text{C}=\text{O}$). For AT, the intensity of the 1740-cm^{-1} bands was lower when compared to the ones from the raw biosorbent, which also happened to BT and ABT, although in greater intensity, since the bands reduced significantly or even disappeared. This phenomenon suggests the hydrolysis of esters and amides to carboxylic acid groups (Pilon & Lavoie, 2011).

According to Chen et al. (2015), the change in the range of $1640\text{--}1600\text{ cm}^{-1}$ may be linked to aromatic, carboxylic and alkenes groups ($\text{C}=\text{O}$ and $\text{C}=\text{C}$), while a change in the peak at 1384 cm^{-1} suggests stretching of nitrates (N-O). Likewise, the range between 1265 and 1220 cm^{-1} can be attributed to vibrations from phenolic groups, carboxylic acids, amines and amides (C-O and C-N). Furthermore, it is possible to identify the stretch at 1270 cm^{-1} (C-O-C) and esters at 1225 cm^{-1} .

The absence of the $\text{C}=\text{O}$ peak at 1740 cm^{-1} in the spectrum after the adsorption process may be associated with the formation of hydrogen bonds after the adsorption of metformin. According to Zhu et al. (2017), this suggests that the formation of $\pi - \pi$ interactions and hydrogen bonds may be the main adsorption mechanism.

Preliminary tests

The influence of initial pH in the process of metformin hydrochloride adsorption was evaluated through

pre-tests by comparing seven pH values (4, 5, 6, 7, 8, 9 and 10) at $25\text{ }^{\circ}\text{C}$ and 100 rpm (tests 1–7 described in Table 1) to evaluate the response that the change in the initial pH generates in the removal capacity for the biosorbent (RW, AT, BT and ABT). After analyzing the results from Table 2, pH 7 was chosen to be used in further tests, since values close to neutral provided a slightly higher removal capacity, so no adjustments were necessary.

In the analyzes related to temperature variation at pH 7 and 100 rpm (tests 8–10 described in Table 1), the adsorption process was evaluated at 25 , 35 and $45\text{ }^{\circ}\text{C}$ for RW, AT, BT and ABT. The removal of the drug showed better results at $25\text{ }^{\circ}\text{C}$ (Table 3) and this temperature was used in further tests.

The evaluation of the adsorption process stirring was carried out at 100 , 150 and 200 rpm (pH 7 and $25\text{ }^{\circ}\text{C}$), according to tests 11–13 presented in Table 1. It was found that the stirring did not significantly influence the adsorption process for any biomass evaluated (RW, AT, BT and ABT), with removal capacities of 2.92 , 6.83 , 8.81 and 14.97 mg g^{-1} , respectively. Therefore, 100 rpm was used for milder stirring and easier operation.

By means of the ANOVA, it was observed that the effect of the temperature was significantly different for all biosorbents tested (RW, AT, BT and ABT) at a 95% confidence level. In contrast, the stirring speed did not have a significant influence on the removal, from a statistical point of view, for the biomasses that underwent the chemical treatments. Thus, the response surfaces (Figure 4) were built for the percentage of drug removal as a function of the initial pH of the solution and temperature.

TABLE 2. Effect of pH in the adsorption process ($C_{\text{initial}}= 100 \text{ mg L}^{-1}$, $T= 25^{\circ}\text{C}$, 100 rpm, $t= 24 \text{ h}$).

RW			AT			BT			ABT		
$\text{pH}_{\text{initial}}$	pH_{final}	$q(\text{mg g}^{-1})$									
4,07	6,88	$2,14 \pm 0,11$	4,03	3,82	$6,40 \pm 0,32$	4,01	7,8	$8,38 \pm 0,42$	4,03	7,64	$13,06 \pm 0,65$
4,95	7	$2,47 \pm 0,12$	5	4,26	$6,85 \pm 0,34$	5,08	7,75	$10,26 \pm 0,51$	5	8,01	$16,32 \pm 0,82$
5,94	7,01	$2,52 \pm 0,13$	6,05	4,33	$6,88 \pm 0,34$	6,02	7,81	$10,72 \pm 0,54$	6,05	8	$16,77 \pm 0,84$
7,04	7	$2,63 \pm 0,10$	6,95	4,45	$7,16 \pm 0,36$	6,93	7,7	$11,57 \pm 0,58$	6,95	7,9	$17,70 \pm 0,85$
8,01	6,98	$2,45 \pm 0,12$	8,14	4,52	$6,99 \pm 0,35$	7,96	7,59	$10,03 \pm 0,50$	8,14	7,74	$16,20 \pm 0,81$
9,03	7	$2,51 \pm 0,13$	9,09	4,5	$6,91 \pm 0,35$	9,09	7,66	$9,63 \pm 0,48$	9,09	7,97	$16,00 \pm 0,82$
10,12	6,96	$2,38 \pm 0,12$	10,02	4,51	$6,50 \pm 0,32$	10,03	7,5	$9,31 \pm 0,47$	10,02	7,87	$15,44 \pm 0,77$

TABLE 3. Effect of the temperature in the adsorption process ($C_{\text{initial}}= 100 \text{ mg L}^{-1}$, 100 rpm, $t= 24 \text{ h}$).

Temperature ($^{\circ}\text{C}$)	$q(\text{mg g}^{-1})$			
	RW	AT	BT	ABT
25	$2,54 \pm 0,10$	$6,33 \pm 0,21$	$12,45 \pm 0,36$	$17,14 \pm 0,27$
35	$2,33 \pm 0,12$	$5,62 \pm 0,01$	$11,93 \pm 0,39$	$15,69 \pm 0,39$
45	$2,01 \pm 0,12$	$5,57 \pm 0,23$	$10,29 \pm 0,09$	$13,01 \pm 0,18$

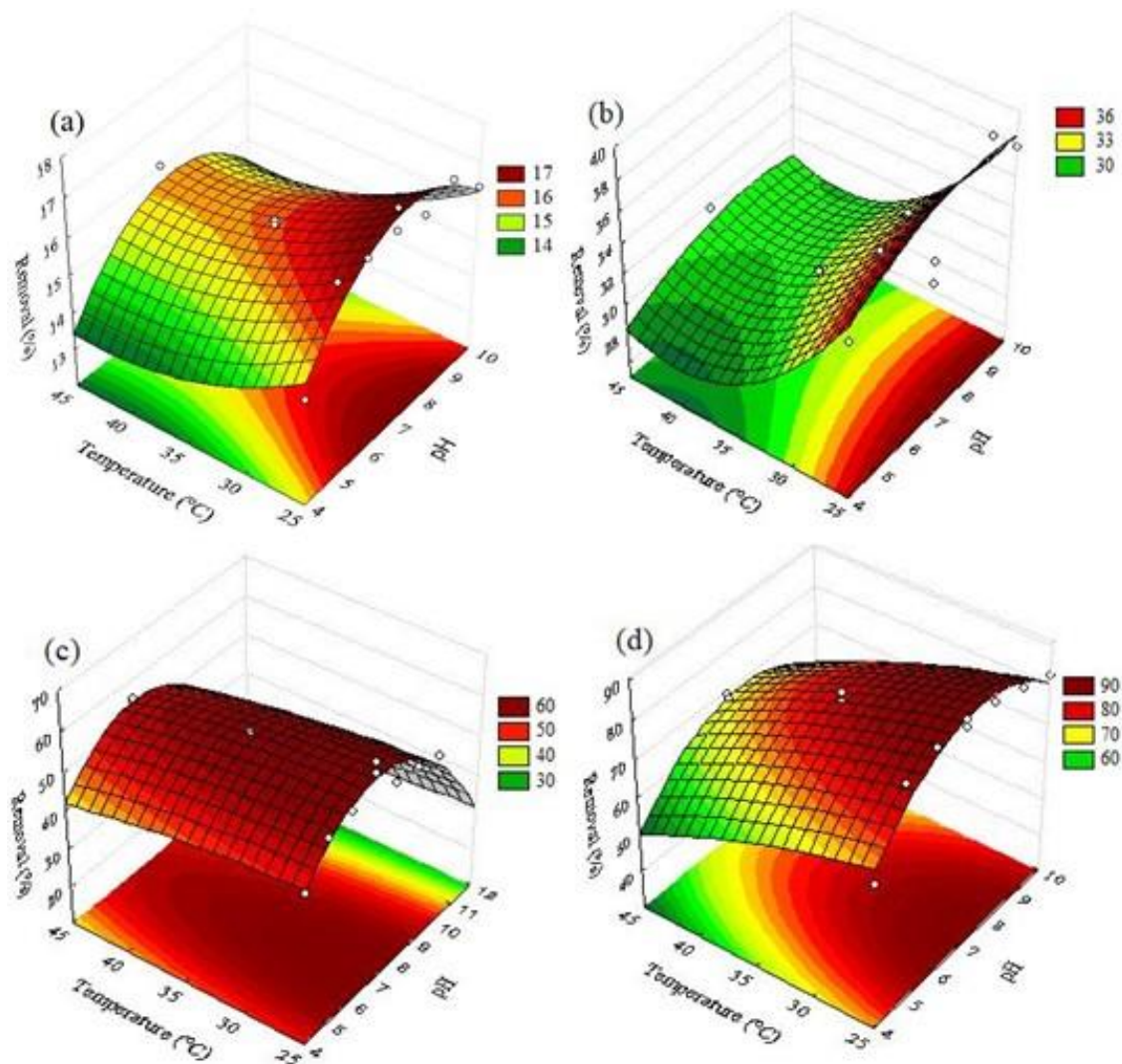


FIGURE 4. Response surface for the percentage of removal as a function of the pH and temperature for biosorbents (a) RW, (b) AT, (c) BT and (d) ABT.

Overall, it is noted that greater drug removal capacities can be reached with pH values close to 7 at $\sim 25\text{ }^{\circ}\text{C}$. For the stirring speed, since there were no significant differences, 100 rpm was used for further experiments. Thus, the preliminary tests indicated that the operating conditions that favor the removal process, among the conditions evaluated, are pH 7, $25\text{ }^{\circ}\text{C}$ and stirring at 100 rpm.

Kinetic tests

The evaluation of biosorption kinetics for peach pit (RW, AT, BT and ABT) was carried out with initial concentrations of 100 and 400 mg L^{-1} under the most favorable sorption conditions for the removal of the drug (pH 7, $25\text{ }^{\circ}\text{C}$ and 100 rpm). Under such conditions, the balance occurred at $\sim 8\text{ h}$, which is a relatively short time. In addition, ABT showed a significant reduction in the equilibrium time (2 h) and an increase in the adsorption capacity, as shown in Figure 5.

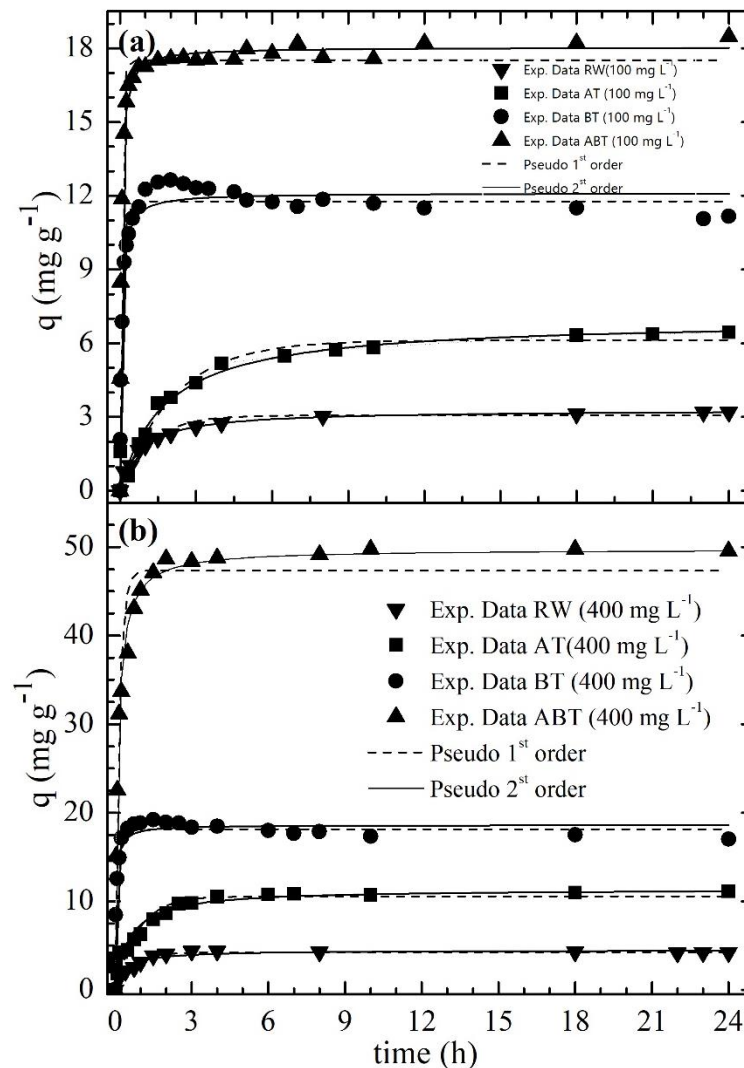


FIGURE 5. Kinetic data for the process of drug adsorption: (a) $C_{\text{initial}}=100\text{ mg L}^{-1}$, $\text{pH}_{\text{initial}}=7$, $T=25\text{ }^{\circ}\text{C}$ and 100 rpm; (b) $C_{\text{initial}}=400\text{ mg L}^{-1}$, $\text{pH}_{\text{initial}}=7$, $T=25\text{ }^{\circ}\text{C}$ and 100 rpm.

The values of the adjusted parameters of the kinetic models are listed in Table 4. Among the evaluated models, the pseudo-second-order model was the one that best fit the experimental data, according to the correlation coefficients (R^2), for the two concentrations evaluated (100 and 400 mg L^{-1}) and for RW, AT, BT, and ABT. According to Ho & McKay (1999), the adjustment takes place by the pseudo-second-order model because it considers a chemisorption step controlling the process and depends on the amount adsorbed on the surface of the adsorbent and in the state of equilibrium.

In the analysis of the kinetic data by the intraparticle diffusion model for the biosorption process, it was found that there is an influence of the chemical treatment of the

biomaterial and the concentration of the drug in the solution, as shown in Figure 6. It is possible to observe sections that present multilinearities, revealing different adsorption zones with different slopes (Módenes et al., 2015b). Three mass transfer zones were established for the tests (100 and 400 mg L^{-1}). A higher diffusion rate was identified in the first zone (Zone I), that is, the first phase of drug sorption occurs on the outer surface of the biosorbent. In Zone II, gradual adsorption occurs with mass transfer in the macropores. In Zone III, adsorption occurs in the micropores and is characterized by intraparticle diffusion. This is followed by the final equilibrium phase. Each zone was linearized by the values of k_{dif} and C , according to Table 5.

TABLE 4. Values of the adjusted parameters of the adsorption kinetic models.

Initial concentration	Kinetic models	Adjustable parameters	Biosorbent			
			RW	AT	BT	ABT
100 mg L ⁻¹	Pseudo-first order	q _e (mg g ⁻¹) qm	3,04 ± 0,08	6,08 ± 0,12	11,77 ± 0,14	17,51 ± 0,18
		k ₁ (h ⁻¹)	0,87 ± 0,08	0,48 ± 0,03	10,07 ± 0,83	14,81 ± 1,18
		R ²	0,9669	0,9860	0,9745	0,9761
	Pseudo-second order	q _e (mg g ⁻¹)	3,29 ± 0,04	6,91 ± 0,16	12,14 ± 0,14	18,05 ± 0,08
		k ₂ (g mg ⁻¹ h ⁻¹)	0,38 ± 0,03	0,08 ± 0,01	1,45 ± 0,15	1,35 ± 0,06
		R ²	0,9946	0,9875	0,9789	0,9960
400 mg L ⁻¹	Pseudo-first order	q _e (mg g ⁻¹) qm	3,17 ± 0,07	10,58 ± 0,49	18,11 ± 0,20	47,33 ± 1,09
		k ₁ (h ⁻¹)	1,47 ± 0,15	1,13 ± 0,21	14,33 ± 1,17	6,19 ± 0,80
		R ²	0,9610	0,8743	0,9789	0,8987
	Pseudo-second order	q _e (mg g ⁻¹)	3,31 ± 0,10	11,37 ± 0,53	18,61 ± 0,27	49,75 ± 0,27
		k ₂ (g mg ⁻¹ h ⁻¹)	0,80 ± 0,16	0,16 ± 0,04	1,31 ± 0,18	0,19 ± 0,01
		R ²	0,9662	0,9077	0,9888	0,9844

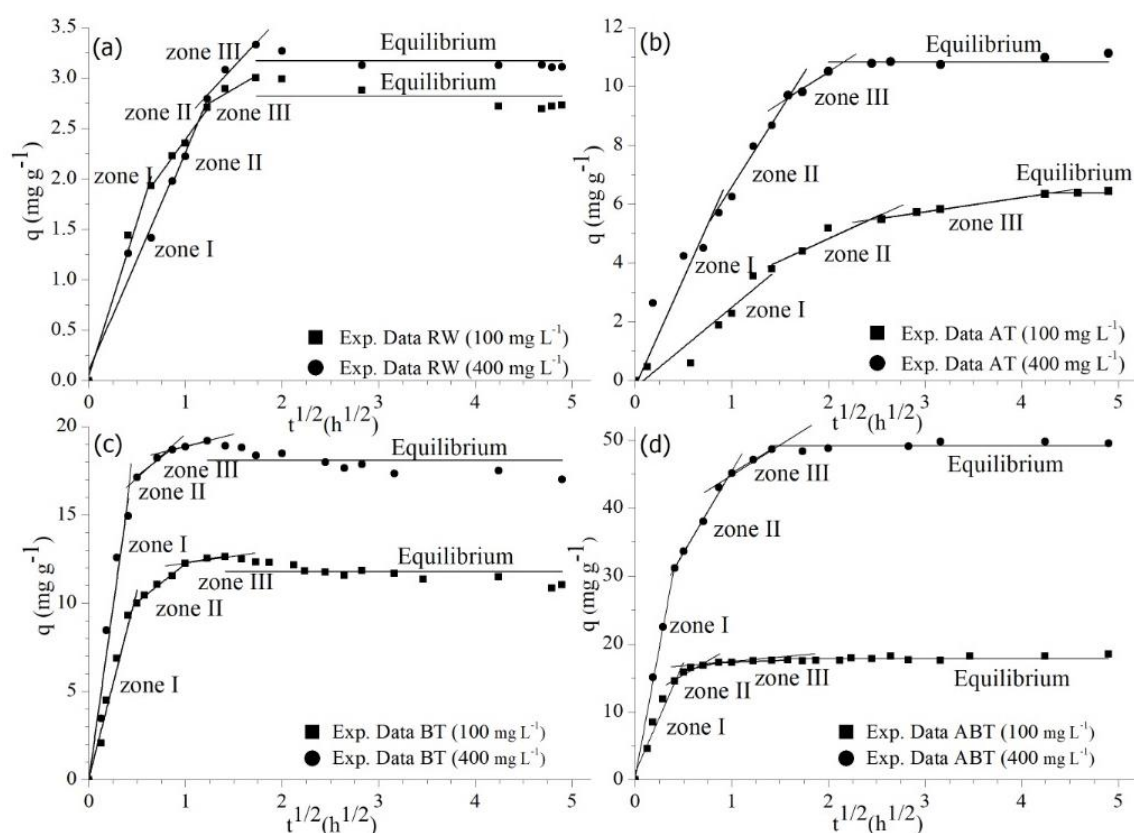


FIGURE 6. Evaluation of kinetic data by the intraparticle diffusion model for drug adsorption by the biosorbent (a) RW, (b) AT, (c) BT and (d) ABT.

By comparing the raw biomass ($\sim 3.17 \text{ mg g}^{-1}$) with the ones after the treatments, it was verified that ABT provided a significant increase in the drug removal capacity of the biosorbent ($\sim 49.14 \text{ mg g}^{-1}$), both on the surface and in the pores, i.e., in the three mass transfer zones.

Equilibrium tests

The adsorption equilibrium data for the biosorbent, shown in Figure 7a, were obtained according to the most favorable conditions obtained in the preliminary tests. To evaluate the model that adequately describes the adsorption

process under study, the Langmuir (1916), Freundlich (1906), Redlich & Peterson (1959), Temkin (1981), Dubinin-Radushkevich (1960) and Toth (1971) isotherms were used. The values of the adjusted parameters are shown in Table 6. The model that best fit the experimental data was the Langmuir isotherm, which provided the highest correlation coefficient (R^2) for all treatment conditions, suggesting that the drug adsorption occurs in the monolayer, with a homogeneous surface.

TABLE 5. Parameters of the intra-particle diffusion model for drug adsorption in the concentrations of 100 and 400 mg L⁻¹. for the RW, AT, BT and ABT biosorbent.

Initial concentration	Diffusion zone	Adjustable parameters	Biosorbent				
			RW	AT	BT	ABT	
100 mg L ⁻¹	Zone I	k _{dif} (mg g ⁻¹ h ^{1/2}) qm	3.05 ± 0.39	2.72 ± 0.35	21.28 ± 1.75	32.31 ± 3.45	
		C ₁ (mg g ⁻¹)	0.05 ± 0.17	-0.22 ± 0.31	0.11 ± 0.53	1.10 ± 1.04	
		R ²	0.9685	0.9074	0.9670	0.9456	
	Zone II	k _{dif} (mg g ⁻¹ h ^{1/2}) qm	1.32 ± 0.08	1.51 ± 0.36	4.34 ± 0.26	3.58 ± 0.74	
		C ₂ (mg g ⁻¹)	1.07 ± 0.07	1.81 ± 0.70	7.90 ± 0.20	14.23 ± 0.50	
		R ²	0.9895	0.8489	0.9854	0.9806	
	Zone III	k _{dif} (mg g ⁻¹ h ^{1/2}) qm	0.56 ± 0.17	0.49 ± 0.03	0.93 ± 0.21	0.58 ± 0.11	
		C ₃ (mg g ⁻¹)	2.06 ± 0.25	4.28 ± 0.09	11.35 ± 0.26	16.74 ± 0.13	
		R ²	0.8285	0.9912	0.9009	0.8771	
	Equilibrium	q _e (mg g ⁻¹)	2.81	6.38	11.80	17.84	
	400 mg L ⁻¹	Zone I	k _{dif} (mg g ⁻¹ h ^{1/2}) qm	3.01 ± 0.16	5.85 ± 1.05	38.98 ± 4.90	76.25 ± 2.21
			C ₄ (mg g ⁻¹)	0.06 ± 0.11	0.78 ± 0.58	0.03 ± 1.20	0.43 ± 0.59
R ²			0.9893	0.8820	0.9396	0.9974	
Zone II		k _{dif} (mg g ⁻¹ h ^{1/2}) qm	2.29 ± 0.63	5.66 ± 0.33	4.32 ± 0.63	24.11 ± 1.57	
		C ₅ (mg g ⁻¹)	0.88 ± 0.78	0.77 ± 0.41	15.03 ± 0.45	21.43 ± 0.84	
		R ²	0.8575	0.9867	0.9578	0.9909	
Zone III		k _{dif} (mg g ⁻¹ h ^{1/2}) qm	0.57 ± 0.30	2.03 ± 0.50	1.38 ± 0.08	8.46 ± 0.21	
		C ₆ (mg g ⁻¹)	3.28 ± 0.51	6.42 ± 0.89	17.50 ± 0.08	36.71 ± 0.25	
		R ²	0.5763	0.8861	0.9936	0.9988	
Equilibrium		q _e (mg g ⁻¹)	3.17	10.83	18.10	49.14	

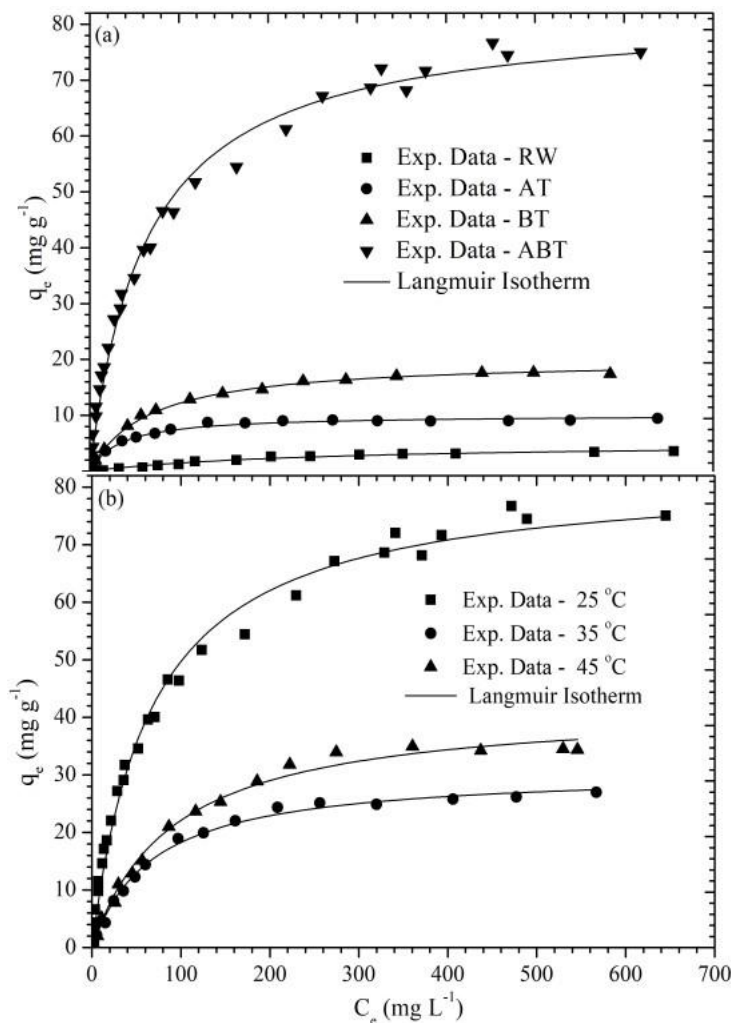


FIGURE 7. Langmuir isotherm adjusted to the equilibrium data of drug adsorption: for (a) RW, AT, BT and ABT biosorbents under the following conditions pH_{initial}=7.0, T=25 °C, 100 rpm and 24h; (b) for the ABT biosorbent at 25, 35 and 45 °C.

It can be seen from the equilibrium data (Figure 7a) that ABT presented a higher adsorption capacity compared to RW, AT and BT. The treatment presented in this work (ABT) increased the maximum biomass adsorption capacity from 5.19 ± 0.34 to 82.54 ± 1.34 mg g⁻¹, according to the q_{\max} parameter obtained from the fit of the Langmuir isotherm to the experimental data. Such an improvement can be attributed to the renewal of the organic surface by the treatment performance, as well as the increase in the specific area and volume of the micropores. This result agrees with the micrographs obtained from scanning electron microscopy, which suggest that, after the treatment, the surface of the biosorbent presented more irregular and heterogeneous characteristics.

Since the ABT was the one that provided the highest adsorption capacity, according to Table 6, as confirmed by the preliminary and kinetic tests, it was used to evaluate the equilibrium at three temperatures (25, 35 and 45 °C). The results are shown in Figure 7b. All equilibrium models were evaluated for the three temperatures used and the parameters estimated are shown in Table 7. According to the correlation coefficient (R²), the Langmuir model was the one that best fit the experimental data for all temperatures evaluated. According to the estimated parameters (Table 7), as well as the data presented in Figure 7b, the best adsorption performance occurred at 25 °C, reaching 82.54 ± 1.34 mg g⁻¹.

TABLE 6. Values of the adjusted parameters of the adsorption equilibrium models.

Isotherms	Adjustable parameters	Biosorbent			
		RW	AT	BT	ABT
Langmuir	q_{\max} (mg g ⁻¹)	$5,19 \pm 0,34$	$10,11 \pm 0,39$	$20,09 \pm 0,69$	$82,54 \pm 1,34$
	b (L mg ⁻¹)	$3,7 \cdot 10^{-3} \pm 5 \cdot 10^{-4}$	$0,03 \pm 0,01$	$0,01 \pm 1,9 \cdot 10^{-3}$	$0,02 \pm 8 \cdot 10^{-4}$
	R ²	0,9798	0,9416	0,9798	0,9926
Freundlich	k_F (L ⁻¹)	$0,11 \pm 3,6 \cdot 10^{-4}$	$1,91 \pm 0,43$	$2,05 \pm 0,48$	$6,99 \pm 0,73$
	n	$1,82 \pm 0,19$	$3,79 \pm 0,59$	$2,81 \pm 0,35$	$2,55 \pm 0,12$
	R ²	0,9321	0,8291	0,918	0,9668
Redlich Peterson	k_{rp} (L g ⁻¹)	$0,01 \pm 1,2 \cdot 10^{-4}$	$0,21 \pm 0,05$	$0,25 \pm 0,04$	$1,74 \pm 0,15$
	a_{rp} (L mg ⁻¹)	$0,01 \pm 1 \cdot 10^{-4}$	$0,01 \pm 0,01$	$0,01 \pm 5,4 \cdot 10^{-3}$	$0,05 \pm 0,01$
	b (L mg ⁻¹)	$1,53 \pm 0,23$	$1,11 \pm 0,09$	$1,09 \pm 0,10$	$0,87 \pm 0,03$
	R ²	0,9785	0,9402	0,9701	0,9917
Temkin	b (L mg ⁻¹)	$0,93 \pm 0,07$	$1,5342 \pm 0,16$	$2,46 \pm 0,30$	$11,96 \pm 0,66$
	k_T (L mg ⁻¹)	$0,06 \pm 0,01$	$0,9575 \pm 0,47$	$1,42 \pm 0,85$	$0,59 \pm 0,12$
Dubinin Radushkevich	R ²	0,9331	0,8512	0,808	0,9137
	$q_{\max,DR}$ (mg g ⁻¹)	$3,32 \pm 0,12$	$8,73 \pm 0,31$	$16,55 \pm 0,58$	$65,12 \pm 2,74$
	β_{sDR} (L mg ⁻¹)	$9,5 \cdot 10^{-7} \pm 1,3 \cdot 10^{-7}$	$5,1 \cdot 10^{-8} \pm 1,3 \cdot 10^{-8}$	$1,8 \cdot 10^{-7} \pm 3,6 \cdot 10^{-8}$	$1,1 \cdot 10^{-7} \pm 2,2 \cdot 10^{-8}$
Toth	R ²	0,9527	0,8957	0,9428	0,9527
	$q_{\max T}$ (mg g ⁻¹)	$3,6508 \pm 0,1744$	$9,3870 \pm 0,4418$	$18,4290 \pm 1,08$	$102,17 \pm 6,52$
	b_T (L mg ⁻¹)	$3,7 \cdot 10^{-4} \pm 2 \cdot 10^{-4}$	$0,02 \pm 4,7 \cdot 10^{-4}$	$0,01225 \pm 2,1 \cdot 10^{-3}$	$0,02 \pm 2 \cdot 10^{-3}$
	n_T	$2,46 \pm 0,55$	$1,58 \pm 0,52$	$1,37 \pm 0,35$	$0,64 \pm 0,06$
	R ²	0,9705	0,9411	0,9792	0,9919

Thermodynamic parameters

The estimation of the thermodynamic parameters (ΔG° , ΔH° and ΔS°) of the biosorption process was evaluated for ABT at 25, 35 and 45 °C. The Gibbs energy was determined by [eq. (12)], where the thermodynamic equilibrium constant (K_{eq}) was approximated by adjusting the Langmuir isotherm (b). The variation in enthalpy and entropy was determined from the slope and intersection with the ordinate axis, respectively, as given by [eq. (13)].

The negative values found for the Gibbs free energy (-19.40, -19.24 and -20.62 kJ mol⁻¹ for 25, 35 and 45 °C, respectively) indicate that the adsorption process was spontaneous. The adsorption reaction was exothermic according to the negative enthalpy (-1.55 kJ mol⁻¹), while the value lower than 40 kJ mol⁻¹ indicates that the adsorption process is of a physical nature. Both conclusions

agree with the results obtained by Zhu et al. (2017). The entropy, which is related to the system order after the adsorption process, presented a negative value (-59.06 kJ mol⁻¹), indicating a decrease in randomness at the solid/solution interface, i.e., the accommodation of the drug occurs in more ordered layers of the surface.

CONCLUSIONS

According to the equilibrium data obtained, the highest adsorption capacity was observed for ABT, with the maximum capacity to remove 75.04 mg g⁻¹ when compared to RW (3.59 mg g⁻¹). From the kinetic study, it was found that the removal process is fast, reaching equilibrium after ~12 h, following the pseudo-second-order kinetic model for all tests performed (RW, AT, BT and ABT). Through the

intraparticle diffusion model, it was found that the variations in the mass transfer zones were proportional to the variation in the concentration of the drug. In addition, it

appears that after the treatment of the biomass, the increase in the ability to remove the drug was proportional both on the surface and in the pores.

TABLE 7. Values of the adjusted parameters of the equilibrium adsorption models for the ABT.

Isotherms	Adjustable parameters	Temperature		
		25 °C	35 °C	45 °C
Langmuir	q_{\max} (mg g ⁻¹)	82,54 ± 1,34	30,88 ± 0,53	42,25 ± 1,32
	b (L mg ⁻¹)	0,0151 ± 1.10 ⁻⁴	0,0110 ± 0,00	0,0146 ± 0,00
	R ²	0,9926	0,9955	0,9872
Freundlich	k_F (L ⁻¹)	6,92 ± 0,73	2,80 ± 0,54	3,03 ± 0,65
	n	2,55 ± 0,13	2,66 ± 0,25	2,48 ± 0,23
	R ²	0,9668	0,9443	0,9382
Redlich Peterson	k_{rp} (L g ⁻¹)	1,74 ± 0,15	0,37 ± 0,02	0,36 ± 0,03
	a_{rp} (L mg ⁻¹)	0,05 ± 0,01	0,01 ± 1.10 ⁻³	1.10 ⁻³ ± 1.10 ⁻⁴
	b (L mg ⁻¹)	0,87 ± 0,03	1,12 ± 0,04	1,16 ± 0,08
Temkin	R ²	0,9917	0,9945	0,9813
	b (L mg ⁻¹)	11,96 ± 0,66	3,97 ± 0,38	5,71 ± 0,58
	k_T (L mg ⁻¹)	0,59 ± 0,12	0,99 ± 0,42	0,55 ± 0,22
Dubinin Radushkevich	R ²	0,9137	0,8639	0,8505
	$q_{\max,DR}$ (mg g ⁻¹)	65,12 ± 2,74	24,44 ± 0,94	31,87 ± 1,43
	β_{sDR} (L mg ⁻¹)	1,1.10 ⁻⁷ ± 2,2.10 ⁻⁸	1,5.10 ⁻⁷ ± 2,7.10 ⁻⁸	1,9.10 ⁻⁷ ± 4,1.10 ⁻⁸
Toth	R ²	0,9527	0,9343	0,9428
	$q_{\max T}$ (mg g ⁻¹)	102,17 ± 6,52	27,94 ± 0,60	37,5505 ± 1,4524
	b_T (L mg ⁻¹)	0,02 ± 2.10 ⁻³	0,01 ± 6.10 ⁻⁴	0,01 ± 7.10 ⁻⁴
	n_T	0,64 ± 0,06	1,42 ± 0,13	1,47 ± 0,22
	R ²	0,9919	0,9945	0,9829

For the equilibrium data, the Langmuir isotherm was the one that best fit the experimental data for all the operating temperatures evaluated, suggesting that the biosorption of the drug occurs in monolayers with q_{\max} estimated for ABT as 82.54 ± 1.34 mg g⁻¹. As for the proposed biomass treatment, compared to RW, there was an increase in the removal capacity of 2, 4 and 16 times after the AT, BT and ABT treatments, respectively. Therefore, the proposed chemical treatment allows the peach pit to pass from an agricultural residue to an efficient biosorbent to be used in the removal of drugs.

ACKNOWLEDGEMENTS

The authors would like to thank the Center of Analysis – UTFPR Campus Pato Branco for the scanning electron microscopy and Fourier transform infrared spectroscopy analyzes.

REFERENCES

Álvarez-Torrellas S, Lovera RG, Escalona N, Sepúlveda C, Sotelo JL, García J (2015) Chemical-activated carbons from peach stones for the adsorption of emerging contaminants in aqueous solutions. *Chemical Engineering Journal* 279:788–798. DOI: <https://doi.org/10.1016/j.cej.2015.05.104>

Álvarez-Torrellas S, Rodríguez A, Ovejero G, García J (2016) Comparative adsorption performance of ibuprofen and tetracycline from aqueous solution by carbonaceous materials. *Chemical Engineering Journal* 283:936–947. DOI: <https://doi.org/10.1016/j.cej.2015.08.023>

Bartrons M, Penuelas J (2017) Pharmaceuticals and personal-care products in plants. *Trends Plant Sci* 22:194–203. DOI 10.1016/j.tplants.2016.12.010

Bazarin G, Módenes AN, Vieira AMG, Borba CE, Espinoza-Quñones FR, Scariotto MC (2019) Tilapia scales: characterization and study of Cu(II) removal by ion exchange with Ca(II). *Separation Science and Technology* 54:1–13. DOI: <https://doi.org/10.1080/01496395.2019.1577260>

Carmalin AS, Lima EC (2018) Removal of emerging contaminants from the environment by adsorption. *Ecotoxicology and Environmental Safety* 150:1–17. DOI: <https://doi.org/10.1016/j.ecoenv.2017.12.026>

Chen Z, Hu TQ, Jang HF, Grant E (2015) Modification of xylan in alkaline treated bleached hardwood kraftpulp as classified by attenuated total-internal-reflection (ATR) FTIR spectroscopy. *Carbohydrate Polymers* 127:418–426. DOI: <https://doi.org/10.1016/j.carbpol.2015.03.084>

- Conrado, NM (2019) Remoção de paracetamol de solução aquosa em carbono ativado. Trabalho de Conclusão de Curso. Universidade Federal Rural Do Semiárido.
- Davranche M, Lacour S, Bordas F, Bollinger JC (2003) An easy determination of the surface chemical properties of simple and natural solids. *Journal of Chemical Education* 80:76–78. DOI: <https://doi.org/10.1021/ed080p76>
- Dubinin MM (1960) The potential theory of adsorption of gases and vapors for adsorbents with energetically nonuniform surfaces. *Chemical Reviews* 60:235–241. DOI: <https://doi.org/10.1021/cr60204a006>
- Espinoza-Quiñones FR, Módenes AN, Câmara AS, Stutz G, Tirão G, Palácio SM, Kroumov AD, Oliveira AP, Alflen VL (2010) Application of high-resolution X-ray emission spectroscopy on the study of Cr ion adsorption by activated carbon. *Applied Radiation and Isotopes* 8:2208–2213. DOI: <https://doi.org/10.1016/j.apradiso.2010.06.006>
- Freundlich H (1906) Over the adsorption in solution (Über die adsorption in Lösungen). *Journal of Physical Chemistry (Zeitschrift für Physikalische Chemie)* 57:385–470.
- Ho YS (2004) Citation review of Lagergren kinetic rate equation on adsorption reactions. *Scientometrics* 59:171–177. DOI: <https://doi.org/10.1023/B:SCIE.0000013305.99473.cf>
- Ho YS, McKay G (1999) Pseudo-second order model for sorption processes. *Process Biochemistry* 34:451–465. DOI: [https://doi.org/10.1016/S0032-9592\(98\)00112-5](https://doi.org/10.1016/S0032-9592(98)00112-5)
- Ho YS, McKay G (2000) The kinetics of sorption of divalent metal ions onto sphagnum moss peat. *Water Research* 34:735–742. DOI: [https://doi.org/10.1016/S0043-1354\(99\)00232-8](https://doi.org/10.1016/S0043-1354(99)00232-8)
- Inyang M, Dickenson E (2015) The potential role of biochar in the removal of organic and microbial contaminants from potable and reuse water: a review. *Chemosphere* 134:232–240. DOI: <http://dx.doi.org/10.1016/j.chemosphere.2015.03.072>
- Jean J, Perrodin Y, Pivot C, Trepo D, Perraud M, Droguet J, Tissot-Guerraz F, Locher F (2012) Identification and prioritization of bioaccumulable pharmaceutical substances discharged in hospital effluents. *Journal Environmental Management* 103:113–121. DOI: <https://doi.org/10.1016/j.jenvman.2012.03.005>
- Lagergren S (1898) About the theory of so-called adsorption of soluble substances. *Kungliga Suensk Vetenskapsakademiens Handlingar* 4:1–39.
- Langmuir I (1916) The Constitution and Fundamental Properties of Solids and Liquids. Part I. Solids. *Journal of the American Chemical Society* 38:2221–2295. DOI: <https://doi.org/10.1021/ja02268a002>
- Larsson DGJ (2014) Pollution from drug manufacturing: review and perspectives. *Philosophical Transactions of the Royal Society B* 369(1656):20130571. DOI: <https://doi.org/10.1098/rstb.2013.0571>
- Maldonado PSV, Montoya VH, Montes-Moránb MA (2016) Plasma-surface modification vs. air oxidation on carbon obtained from peach stone: Textural and chemical changes and the efficiency as adsorbents. *Instituto Applied Surface Science* 384:143–151. DOI: <http://dx.doi.org/10.1016/j.apsusc.2016.05.018>
- Markovic S, Stankovi A, Lopicic Z, Lazarevi S, Stojanovi M, Uskokovi S (2015) Application of raw peach shell particles for removal of methylene blue. *Journal of Environmental Chemical Engineering* 3:716–724. DOI: <http://dx.doi.org/10.1016/j.jece.2015.04.002>
- Módenes AN, Espinoza-Quiñones FR, Santos GHF, Borba CE, Rizzutto MA (2013) Assessment of metal sorption mechanisms by aquatic macrophytes using PIXE analysis *Journal of Hazardous Materials* 261:148–154. DOI: <http://dx.doi.org/10.1016/j.jhazmat.2013.07.020>
- Módenes AN, Espinoza-Quiñones FR, Colombo A, Geraldi CL, Trigueros DEG (2015a) Inhibitory effect on the uptake and diffusion of Cd²⁺ onto soybean hull sorbent in Cd-Pb binary sorption systems. *Journal Environmental Management* 154:22–32. DOI: <http://dx.doi.org/10.1016/j.jenvman.2015.02.022>
- Módenes AN, Espinoza-Quiñones FR, Geraldi CAQ, Manenti DR, Trigueros DEG, Oliveira AP, Borba CE, Kroumov AD (2015b) Assessment of the banana pseudostem as low-cost biosorbent for removal of the reactive blue 5G dye. *Environmental Technology* 36:2892–2902. DOI: <http://dx.doi.org/10.1080/09593330.2015.1051591>
- Módenes AN, Hinterholz CL, Neves CV, Sanderson K, Trigueros DEG, Espinoza-Quiñones FR, Borba CE, Steffen V, Scheufele FB, Kroumov AD (2019) A new alternative to use soybean hulls on the adsorptive removal of aqueous dyestuff. *Bioresource Technology Reports* 6:175–182. DOI: <https://doi.org/10.1016/j.biteb.2019.03.004>
- Muñoz-González Y, Arriagada-Acuña R, Soto-Garrido G, García-Lovera R (2008) Activated carbons from peach stones and pine sawdust by phosphoric acid activation used in clarification and decolorization processes. *Journal of Chemical Technology Biotechnology* 84:39–47. DOI: <https://doi.org/10.1002/jctb.2001>
- Niemuth NJ, Jordan R, Crago J, Blanksma C, Johnson R, Klaper RD (2015) Metformin exposure at environmentally relevant concentrations causes potential endocrine disruption in adult male fish. *Environmental Toxicology and Chemistry* 34(2):291–296. DOI: <https://doi.org/10.1002/etc.2793>
- Oliveira AP, Módenes AN, Bragião ME, Hinterholz CL, Trigueros DEG, Bezerra IGO (2018) Use of grape pomace as a biosorbent for the removal of the Brown KROM KGT dye. *Bioresource Technology Reports* 2:92–99. DOI: <https://doi.org/10.1016/j.biteb.2018.05.001>
- Pilon G, Lavouie JM (2011) Characterization of switchgrass char produced in torrefaction and pyrolysis conditions. *BioResources* 6:4824–4839.

- Redlich O, Peterson DL (1959) A useful adsorption isotherm. *Journal of Physical Chemistry* 63:1024–1026. DOI: <https://doi.org/10.1021/j150576a611>
- Rezaee A, Pourtaghi GH, Khavanin A, Mamoozy RS, Ghaneian MT, Godini H (2008) Photocatalytic decomposition of gaseous toluene by TiO₂ nanoparticles coated on activated carbon. *Iranian Journal of Environmental Health Science & Engineering* 5:305–310.
- Ribeiro C, Scheufele FB, Espinoza-Quiñones FR, Módenes AN, Vieira MGA, Kroumov AD, Borba CE (2018) A comprehensive evaluation of heavy metals removal from battery industry wastewaters by applying bio-residue, mineral and commercial adsorbent materials. *Journal of Materials Science* 53:7976–7995. DOI: <https://doi.org/10.1007/s10853-018-2150-6>
- Rigueto CVT, Piccin JS, Dettme A, Rosseto M, Dotto GL, Schmitz APO, Perondi D, Freitas TSM, Loss RA, Geraldi CAQ (2020) Water hyacinth (*Eichhornia crassipes*) roots, an amazon natural waste, as an alternative biosorbent to uptake a reactive textile dye from aqueous solutions. *Ecological Engineering* 150:105817. DOI: <https://doi.org/10.1016/j.ecoleng.2020.105817>
- Scheufele FB, Módenes AN, Borba CE, Ribeiro C, Espinoza-Quiñones FR, Bergamasco R, Pereira NC (2016) Monolayer-multilayer adsorption phenomenological model: Kinetics, equilibrium and thermodynamics. *Chemical Engineering Journal* 284:1328–1341. DOI: <https://doi.org/10.1016/j.cej.2015.09.085>
- Scheufele FB, Staudt J, Ueda MH, Ribeiro C, Steffen V, Borba CE, Módenes AN, Kroumov AD (2019) Biosorption of direct black dye by cassava root husks: Kinetics, equilibrium, thermodynamics and mechanism assessment. *Journal of Environmental Chemical Engineering* 7:103533. DOI: <https://doi.org/10.1016/j.jece.2019.103533>
- Shakoor MB, Niazi NK, Bibi I, Shahid M, Saqib ZA, Nawaz MF, Shaheen SM, Wang H, Tsang DCW, Bundschuh J, Ok YS, Rinkleb J (2019) Exploring the arsenic removal potential of various biosorbents from water. *Environment International* 123:567–579. DOI: <https://doi.org/10.1016/j.envint.2018.12.049>
- Tan X, Liu Y, Zeng G, Wang X, Hu X, Gu Y, Yang Z (2015) Application of biochar for the removal of pollutants from aqueous solutions. *Chemosphere* 125:70–85. DOI: <http://dx.doi.org/10.1016/j.chemosphere.2014.12.058>
- Temkin DE (1981) Interface kinetics in the growth of two component crystals. *Journal of Crystal Growth* 52:299–310. DOI: [https://doi.org/10.1016/0022-0248\(81\)90209-8](https://doi.org/10.1016/0022-0248(81)90209-8)
- Toth J (1971) State equations of the solid gas interface layer. *Acta Chimica Academiae Scientiarum Hungaricae* 69:311–317.
- USP (2012) Official Monographs. Metformin, USP 35, The United States Pharmacopeial Convention. Available: https://online.uspnf.com/uspnf/document/GUID-BE09CDF5-9F23-41EC-9856-7C88487236E2_1_en-US?highlight=metformin. Accessed Apr 4, 2019.
- Weber WJ, Morris JC (1963) Kinetics of adsorption on carbon from solution. *Journal of the Sanitary Engineering Division* 89:31–60.
- Yan J, Lan G, Qiu H, Chen C, Liu Y, Du G, Zhang J (2018) Adsorption of heavy metals and methylene blue from aqueous solution with citric acid modified peach stone. *Separations Science and Technology* 53:1678–1688. DOI: <https://doi.org/10.1080/01496395.2018.1439064>
- Zhu S, Liu Y, Liu S, Zeng G, Jiang L, Tan X, Zhou L, Zeng W, Li T (2017) Yang C. Adsorption of emerging contaminant metformin using graphene oxide. *Chemosphere* 179:20–28. DOI: <http://dx.doi.org/10.1016/j.chemosphere.2017.03.0>